Opposing Effects on $Na_V1.2$ Function Underlie Distinction Between Autism Spectrum Disorder and Infantile Seizures Phenotypes in Individuals With *SCN2A* Variants

Supplement 1

Supplemental Methods

Literature search

All papers with "*SCN2A*" in their title or abstract were identified using PubMed and reviewed to identify *SCN2A* variants and associated phenotypes. In addition, published exome analyses of epileptic encephalopathy, developmental delay, intellectual disability, and autism spectrum disorder were searched for *SCN2A* variants. Copy number variants (CNVs) were only included if they did not overlap *SCN1A*. The results are shown in Table S1.

Genetic analysis

SCN2A variants were annotated using the Bamotate script (1) and plotted on $Na_V1.2$ using an in-house script (Fig. 1). The variants were also annotated against bioinformatic tools that predict functional impact (e.g. polyphen2, CADD). No distinction was observed between the missense variants related to infantile seizures or ASD/developmental delay using these methods (Fig. S1).

Cell culture and transfection

Human *SCN2A* wild type (D-Splice variant) or mutated *SCN2A* cDNA were cloned into a pcDNA 3.1(+)IRES GFP vector (Addgene 51406) for fluorescently targeted recording (Genscript). A second pcDNA3.1 vector containing SCN1B (+)IRES SCN2B was co-transfected (Genscript). All constructs were verified with sequencing and submitted for distribution

(Addgene IDs: 84761-84770, 86393, 86394). Human embryonic kidney cells (HEK293, American Type Culture Collection, mycoplasma free) were maintained in 90% DMEM (Invitrogen) and 10% fetal bovine serum; cells were split twice a week and incubated on 3.5 cm dishes prior to transfection. Cells were transfected when cells covered 70-90% of the surface. The transfection cocktail included 500 ng/500 mL of *SCN2A*/eGFP plasmid, 70 ng/500 mL of SCN1B/SCN2B plasmid, and 10 µL/500 mL of Lipofectamine 2000 (Invitrogen). For co-expression, 250 ng/500 mL of each variant was used. Cells were incubated for 16-24 hours at 37ºC and plated for experiments 24 hours post transfection.

Electrophysiology

Whole-cell voltage-clamp recordings were made 4-24 hours after plating. Recordings were made only from isolated, GFP-positive cells at 25ºC using 2-3 MΩ pipettes (Schott 8250). Data were acquired at 50-100 kHz and filtered at 20 kHz (90% series resistance compensation) using a 700B amplifier (Molecular Devices). Internal solution contained (in mM): 110 CsF, 10 NaCl, 20 EGTA, 10 HEPES ~290 mOsm (pH 7.20 with CsOH). Recording solution contained (in mM): 135 NaCl, 4.5 KCl, 2 CaCl, $MgCl_2$ 1, 10 HEPES ~302 mOsm (pH 7.4 with NaOH). In a subset of experiments, a K-gluconate based internal solution was used (in mM): 113 K-Gluconate, 9 HEPES, 4.5 $MgCl_2$, 14 Tris2-phosphocreatine, 4 Na_2-ATP, 0.3 tris-GTP, and 0.1 EGTA.

To assess voltage dependent activation, voltage was stepped from -120 mV to a range from -80 to +80 mV (5 mV increments, 10 ms duration). Peak currents were fitted with $f(V_m) = G_{max}\frac{(V_m\text{-}V_{rev})}{1+exp\frac{V_{0.5}-V_m}{s}}$, where G_{max}: maximal conductance, V_{rev}: reversal potential, $V_{1/2}$: half-maximal activation, *s*: slope. To minimize voltage error, recordings were excluded from subsequent analysis if the measured reversal potential deviated from theoretical (+65.7 mV) by ±8 mV. Peak currents were fitted to a Boltzmann to calculate conductance (G=1/(1 + exp [−(V_m – $V_{0.5}$/k]), G:

norm. conductance, *k*: slope). Voltage dependent inactivation was assessed with 10 ms pulses from -130 to -20 mV proceeded by a 1.4 second holding voltage ranging from -130 to -15 mV (5 mV increments). Channel conductance was calculated from nonstationary fluctuation analysis of steps from -120 to between -15 to +10 mV, (5-10 mV increments, 10-20 trials each) using $\sigma^2(I)=iI-(I^2 / N)$, where σ^2: variance; *i*: single channel current; I: average current; *N*: number of channels. Conductance was calculated from the slope of a line fit across *i* vs. driving force. Inactivation tau was calculated with single exponential fits between 5-95% of the peak current at each voltage. Leak was corrected with P/4 protocols and data was corrected for junction potential.

Immunohistochemistry

Cells were fixed with a 1% Paraformaldehyde (PFA) in phosphate buffered saline (PBS; calcium-, magnesium-free, with 0.04% EDTA) for one hour. PFA was removed and rinsed with PBS before incubating in a permeabilizing blocking solution (10% Normal Donkey Serum, 2% Triton-X; in PBS) for one hour. This blocking solution was then removed and replaced with a mouse Pan-Na_V1 primary antibody (Neuromab 75-405, purified, RRID:AB_2491098) at 1:1000 in solution (1% Normal Donkey Serum, 1% Triton-X) and left to incubate overnight at 4°C. After rinsing with PBS and blocked as above, blocking solution was replaced with an Alexa-Fluor 594 anti-mouse secondary (Invitrogen A-21137) and an Alexa-Fluor 488 anti-GFP conjugate (Invitrogen A-21311) at 1:500 in solution (1% Normal Donkey Serum, 1% Triton-X) for two hours. After rinsing with PBS, coverslips were mounted on slides with Prolong Gold anti-fade media containing DAPI (Thermo Fisher). Single optical sections through the cell centers were acquired on a Nikon Spectral confocal (60x, 1.4 NA oil objective). For TIRF imaging, cells were plated on glass-bottomed 35 mm plates and Alexa-Fluor 594 anti-mouse was replaced with Alexa-Fluor 555 anti-mouse and imaged on a Nikon TIRF microscope (100x, 1.49 NA oil objective). Here, cells were maintained in PBS following final washes. To analyze surface

density of Na_V staining in conducting variants, cells expressing WT, D12N, D82G, and T1420M constructs were run in parallel, and surface staining was analyzed blind. Regions of interest (ROI) were drawn around cells, and mean red fluorescence (Pan-Na_V1) was measured. This was divided by the green/GFP fluorescence in the same ROI to normalize for transfection level. Both Na_V and GFP signals were corrected for background staining by subtracting mean red and green intensities outside ROI bounds.

Compartmental modeling

Simulations were implemented in a pyramidal cell model using the NEURON environment (2), where “Na” and “Nax” channels represented $Na_V1.2$ and $Na_V1.6$, respectively [8 state model: (3)]. Neuronal morphology, channel distribution, and baseline channel kinetics were identical to the published model, except for one condition: in the distal AIS of the adult model, $Na_V1.2$ gbar was explicitly set to 0 (gbar was undefined in the distal AIS in the original model). ASD/BIFS mutations were modeled as changes relative to this baseline. These changes were implemented at 25ºC to match recording configurations. Models were run at 33ºC, with kinetics scaled by the Q10 factor within the model. Manipulations were made only to axonally-localized channels. Developing pyramidal cells were modeled by replacing Nax/$Na_V1.6$ channels in the distal AIS and axonal nodes with Na/$Na_V1.2$ channels. PTV/non-conducting variants were modeled by changing the overall channel conductance from 100% to 50% in 5% increments. Model parameters for all other variants are reported in Table S3. Threshold was defined as the point at which dV/dt exceeded 38 V/s. All models have been submitted for distribution at modelDB.

D12N was modeled as a 35% reduction in $\tau_{inactivation}$. T1420M was modeled as a 16% reduction in $\tau_{inactivation}$ and a 65% reduction in the affected allele’s channel density (net density reduction combining affected and unaffected allele: 32.5%). Because there was no experimental consensus whether D82G surface expression was altered, it was modeled in two ways: as a +5

mV shift in voltage-dependent activation alone (D82G V_a), and as an activation shift with a 63% reduction in the affected allele's density (D82G V_a-#). Further, because some degree of allelic compensation may occur, we modeled PTVs as a range of $Na_V1.2$ expression, from 100% to 50% of normal levels. Because non-conducting missense mutations tend to occur within the pore and not in any cytosolic region associated with membrane trafficking or scaffolding (4, 5), resultant channels traffic to the membrane (Fig. S2) and likely compete for space with WT channels, reducing total sodium conductance across the membrane (Fig. 2B, WT/R379H co-expression). Therefore, we modeled cells heterozygous for non-conducting variants as equivalent to those containing 50% of WT channels.

Statistics

Enrichment of *SCN2A* variants within $Na_V1.2$ domains was assessed using a two-sided binomial exact test (Fig. 1C and text). Differences in non-verbal IQ between ASD cases in the Simons Simplex Collection were assessed using a two-sided Wilcoxon Signed Rank Test. Electrophysiological and TIRF imaging data were reported as mean±SEM in the main text. Unless otherwise noted, data were analyzed using a Kruskal-Wallis test, then a Mann-Whitney post-hoc test with Holm-Šídák correction for multiple comparisons. $p<0.05$ was considered significant.

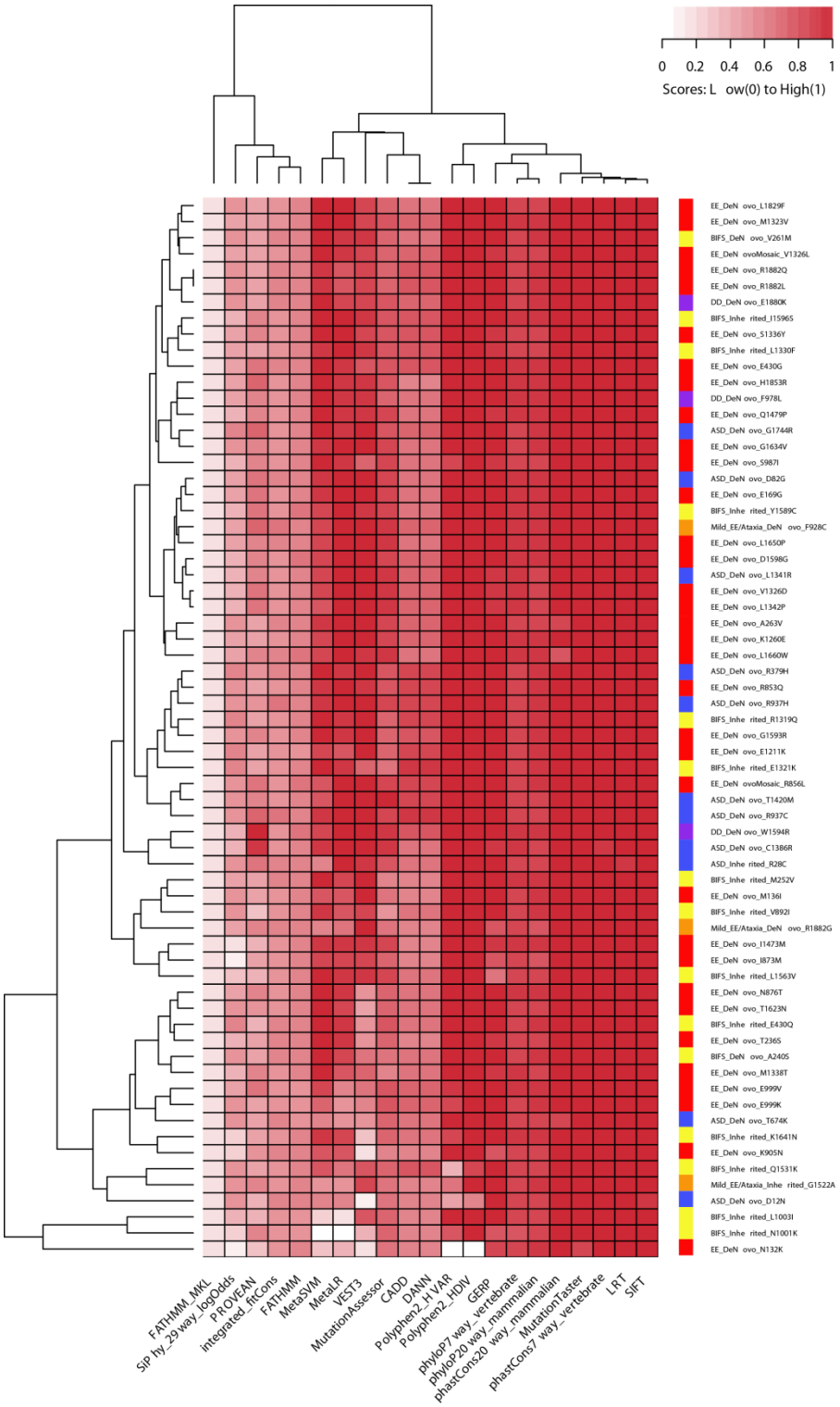

Figure S1: Heatmap of bioinformatics measure of severity for *SCN2A* variants. Corresponds to Main Figure 1. Twenty-one bioinformatic predictors of variant severity were applied to the missense variants from Table S1. Both severity scores and variants were ordered using hierarchical clustering and the results plotted as a heatmap in which red represents high predicted severity and white represents low predicted severity. Of note, there was no consistent pattern distinguishing variants by phenotype.

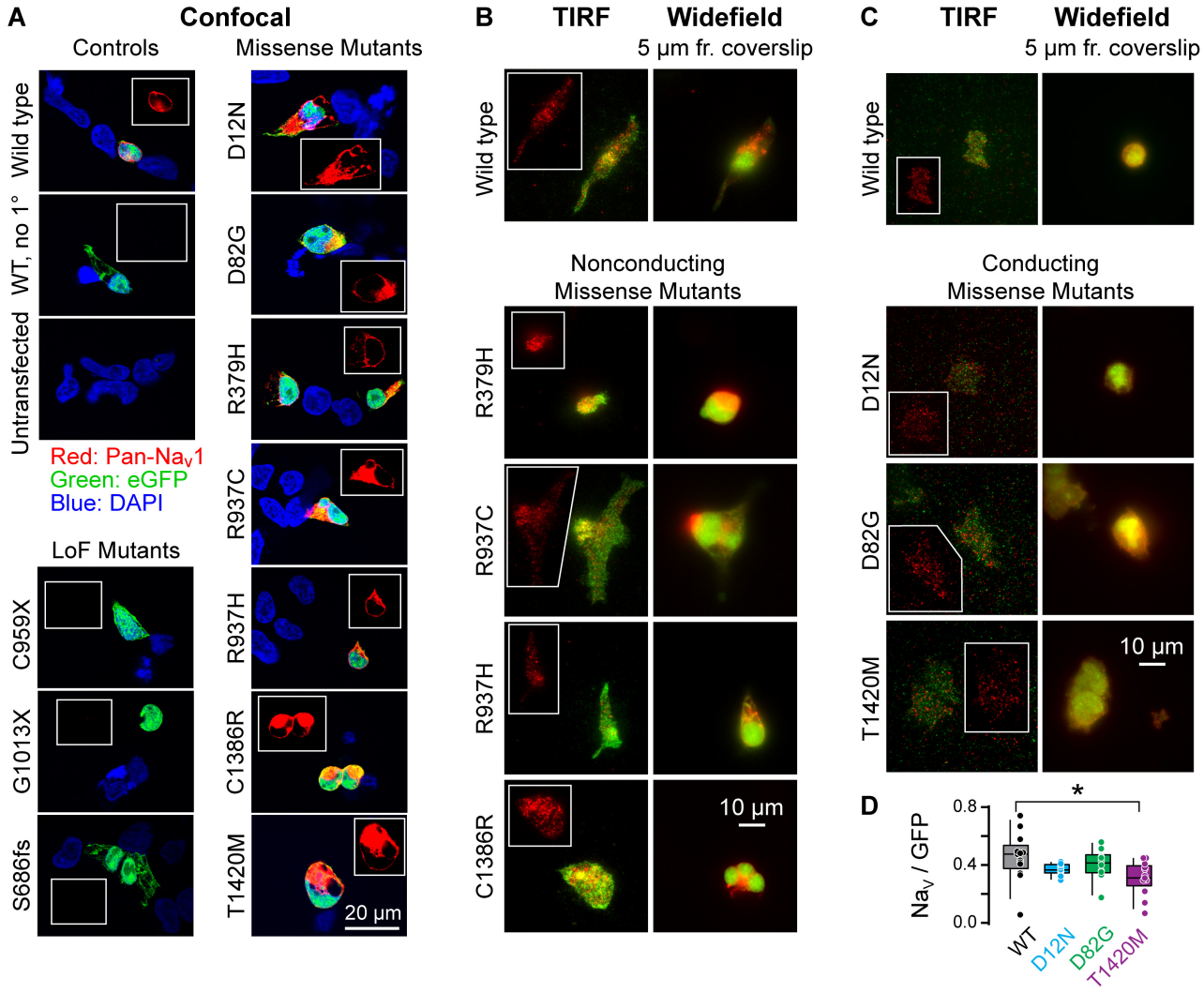

Figure S2: Cellular localization of mutated $Na_V1.2$ channels.
Corresponds to Main Figure 2

A. Single confocal sections transecting cell midlines for all constructs studied. Blue: DAPI, Green: eGFP, Red: Na_V. Insets detail the red channel only, centered on a GFP^+ cell.

B. Left, total internal fluorescence (TIRF) at the cell surface details membrane-associated NaV-staining in WT and non-conducting missense *SCN2A* variants. Green: eGFP, Red: Na_V. Insets detail red channel only. Right, widefield fluorescence of same cells acquired 5 µm from TIRF focal plane, detailing cell morphology more comparable to confocal images in A.

C. Same as B, but for conducting missense variants. Cells were transfected and stained in parallel with WT channels (top).

D. Quantification of NaV intensity, normalized to GFP intensity within cell. Background fluorescence subtracted. All variants were processed in parallel. Data presented as in Figure 2C. Asterisk: p = 0.006.

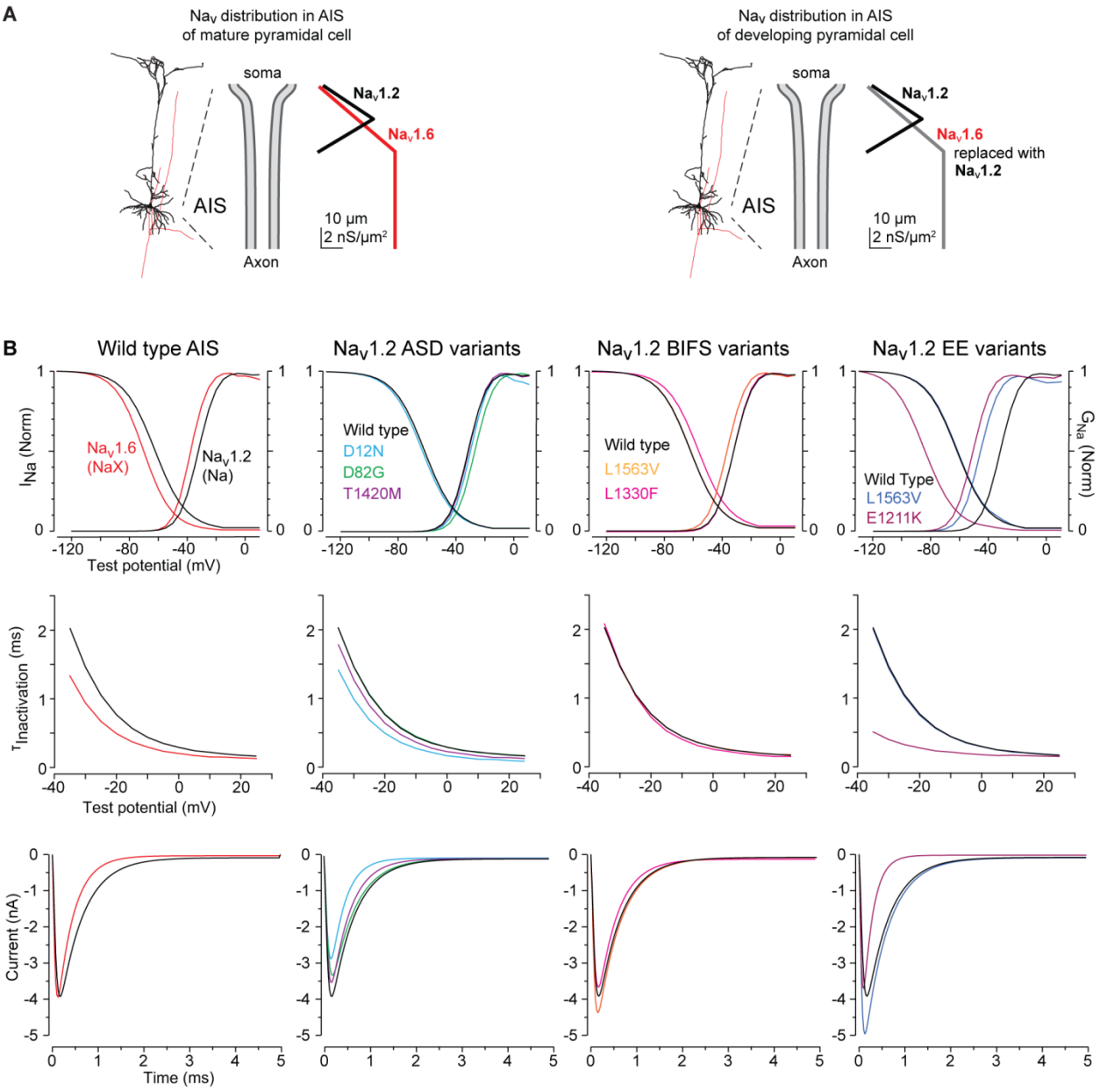

Figure S3: Voltage dependence and kinetics of modeled variants.
Corresponds to Main Figure 3

A. Distribution of sodium channel isoforms in AIS of mature (left) and developing (right) pyramidal cell model.

B. Steady state activation and inactivation (top), inactivation tau (middle, 1-99% of decay), and representative current (bottom, -130 to -15 mV voltage step) for each variant. Data are color coded, with WT in black in each case.

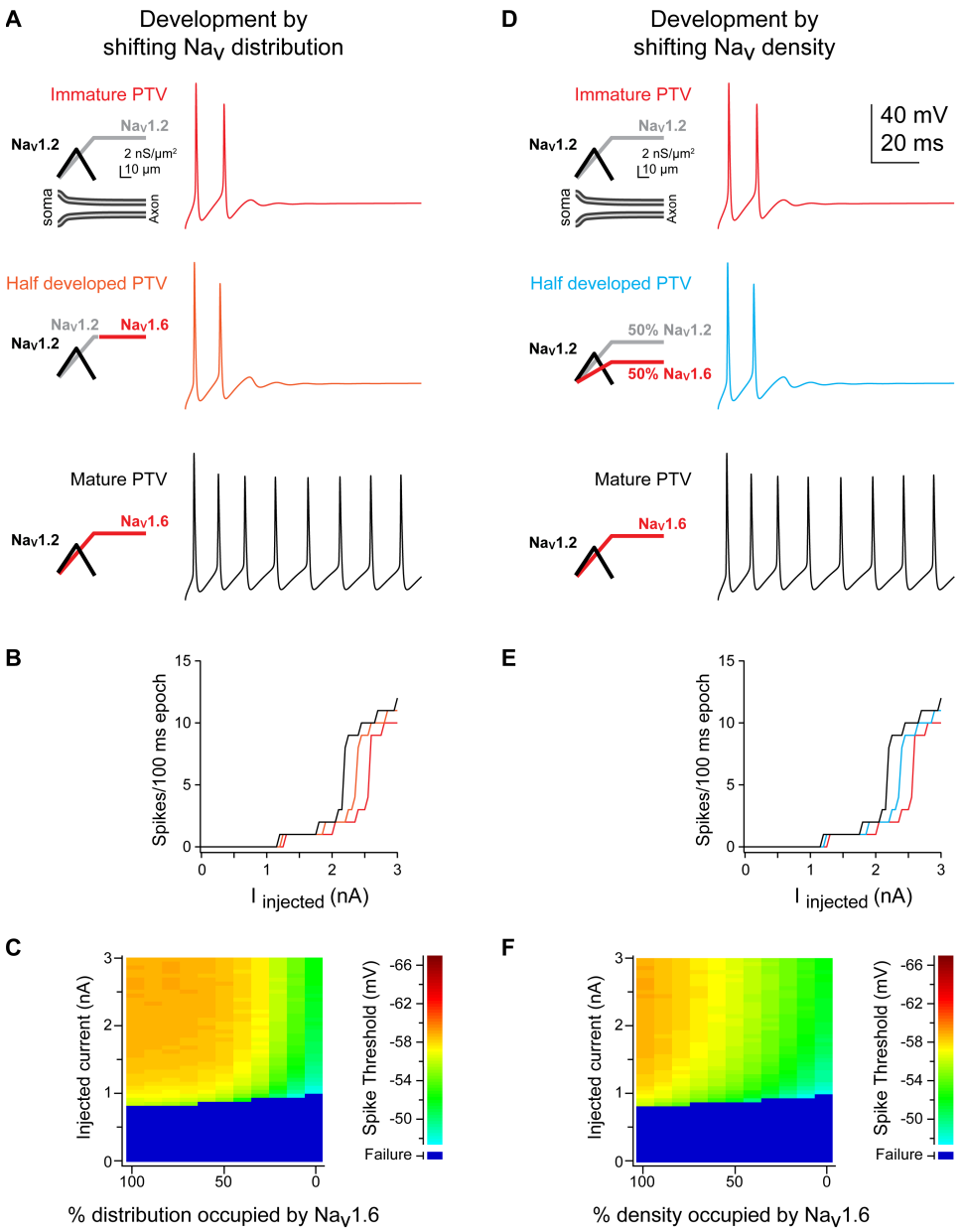

Figure S4: Effects of developmental incorporation of $Na_V1.6$ on neuronal excitability in SCN2A+/- cells. Corresponds to Main Figure 3

A. Spiking generated with 2.2 nA somatic current in SCN2A PTV variant through development. Conditions where no $Na_V1.6$, half of its distribution, and full $Na_V1.6$ expression levels are shown. All traces begin at -78 mV.

B. Number of spikes evoked in 100 ms epoch with varying somatic current injections. PTV is from 50% reduction model. Data are color coded as in **A**.

C. Spike threshold with varying levels of $Na_V1.6$ in the AIS, from fully developed (100% incorporation of $Na_V1.6$) to immature (0%). Colored scale bar corresponds to spike threshold of the first spike observed in each trace; dark blue are conditions in which no spikes were generated.

D-F. Same as **A-C**, but modeling $Na_V1.6$ development as a gradual replacement of $Na_V1.2$ density along the entire distribution area of mature $Na_V1.6$.

Table S1: *SCN2A* Variants
Corresponds to Main Figure 1

See Supplement 2 (Excel file).
A literature search identified 148 variants in *SCN2A*. This table lists the variants, phenotypes, and annotation data with one line per variant. The table has the following columns:

1) Phenotype: Epileptic encephalopathy (EE) defined as seizures before 12mths and moderate to severe developmental delay. Mild EE or sporadic ataxia (Mild_EE/Ataxia) defined as seizures before 12mths mild developmental delay or episodic ataxia. Benign Infantile Familial Seizures (BIFS) defined as seizures before 12mths, remission of seizures before 2yrs and no neurological sequelae. Autism Spectrum Disorder (ASD) defined as no seizures before 12mths and ASD symptoms. Developmental Delay defined as no seizures before 12mths and developmental delay without a record of ASD symptoms. Schizophrenia defined as no seizures before 12mths and schizophrenia. Unclear, defined as lacking sufficient data to clearly fit into one of the prior categories. Other, defined as a diagnosis that differs from one of the previous groups.
2) Variant: The amino acid residue that contains the variant (e.g. R379H).
3) Type: Whether the variant is a protein truncating variant (PTV), missense, deletion, or duplication.
4) Inheritance: Whether the variant is *de novo* (not present in parents), *de novo* mosaic (present in fewer than 50% of cells in the index case), *de novo* germline mosaic (not present in parents but observed in multiple siblings), inherited, unknown.
5) Domain: The domain of $Na_V1.2$ in which the variant is located: N terminus (N-term), Transmembrane segment (e.g. TM4), linker between transmembrane segments (e.g. TM3-4), Pore-loop, Cystoplasmic linker between repeats, C terminus (C-term),
6) Repeat: Whether the variant is in $Na_V1.2$ repeat I, II, III, or IV.
7) Sex: Male (M) or Female (F); unknown is indicated by a period.
8) Age: Age of the index case in days (d), months (m), or years (y); unknown is indicated by a period.
9) Seizures: Yes (Y) or No (N); unknown is indicated by a period.
10) Seizure_type: Description of seizures types; unknown is indicated by a period.
11) Age_of_onset: Age of seizure onset in days (d), months (m), or years (y); unknown is indicated by a period.
12) Age_of_remission: Age of medication free seizure remission in days (d), months (m), or years (y); unknown is indicated by a period.
13) ASD: Presence of autistic symptoms: Yes (Y) or No (N); unknown is indicated by a period.
14) DevDelay: Presence of developmental delay: Yes (Y), No (N), Severe, Moderate, Mild; unknown is indicated by a period.
15) Other: Other diagnoses.
16) SampleID: Sample ID where given; unknown is indicated by a period.
17) Chr: Chromosome.
18) Pos_hg19: Genomic coordinate of the variant in genome build hg19.
19) Ref: Reference allele in VCF format. For copy number variants the stop position genomic coordinate is given.
20) Alt: The alternate allele in VCF format.

21) Type: Single nucleotide variant (SNV), insertion/deletion (Indel), Deletion, or Duplication.
22) Source: First author and year of paper variant was described in.
23) Source(PMID): Pubmed ID of paper variant was described in.
24) FunctionalDataSource: First author and year of paper describing electrophysiological characterization of the variant.
25) FunctionalDataSourcePMID: PubMed ID of paper describing electrophysiological characterization of the variant.
26) Gene: Genes overlapping with the variant.
27) Effect: Effect of the variant on the gene.
28) Initial_Codon: Triplet codon from the reference allele.
29) Initial_AA: Amino acid from the reference allele.
30) New_Codon: Triplet codon from the alternate allele.
31) New_AA: Amino acid from the alternate allele.
32) AA_Change: Reference amino acid, Amino acid number, Alternate amino acid.
33) Total_AA: Number of amino acids in the protein.
34) BP_Change: Reference nucleotide, Nucleotide number in processed mRNA, Alternate nucleotide.
35) Exon_Count: Exon in which the variant is located.

37 to 59) Bioinformatic severity scores (Fig. S1).

Table S2: *SCN2A* Variant Electrophysiology Summary
Corresponds to Main Figure 2

See Supplement 2 (Excel file).
This table summarizes results of all electrophysiological studies of SCN2A variants. Note that some variants have been assessed several times by different groups and are grouped by background shade in rows. Data from this manuscript are included. The table has the following columns:

1) Variant: The amino acid residue that contains the variant (e.g. R379H).
2) Type: Whether the variant is a protein truncating variant (PTV), missense, deletion, or duplication.
3) Phenotype: identical to Phenotype in Table S1.
4) MutationSource: identical to Table S1.
5) MutationSourcePMID: identical to Table S2.
6) FunctionalDataSource: source of electrophysiological characterization.
7) FunctionalDataSourcePMID: PMID of electrophysiological characterization.
8) FunctionalData: Summary of main effects reported in Source.
9) FundtionalRecodingConditions: Expression system and conditions are summarized.
10) FunctionalDataInterpretation: Whether variant is reported to result in hyperexcitability (GoF), hypoexcitability (LoF), or no change in channel function. Interpretations supported by modeling data are noted.

Table S3: Modeling parameters for variants studied. Corresponds to Main Figure 3.
Only adjusted parameters are described here. Note that changes to vShift affect both activation and inactivation, whereas vShift_inactivation affects only inactivation.

Variant	Category	vShift	vShift_inact	gbar scale factor	ah scale factor	bh scale factor
Wild Type		10	10	1	1	1
D12N	ASD	13	17	1	1	3
D82G	ASD	15	5	1	1	1
T1420M	ASD	11	14	0.3	1	1.63
L1563V	BIFS	5	15	1	1	1
L1330F	BIFS	10.4	11.5	1	1.8	1.3
E1211K	EE	-8.4	6	1	1	1
I1473M	EE	-5	25	1	1	1

Supplemental References

1. Sanders SJ, He X, Willsey AJ, Ercan-Sencicek AG, Samocha KE, Cicek AE, et al. (2015): Insights into Autism Spectrum Disorder Genomic Architecture and Biology from 71 Risk Loci. *Neuron*. 87:1215-1233.
2. Hallermann S, de Kock CP, Stuart GJ, Kole MH (2012): State and location dependence of action potential metabolic cost in cortical pyramidal neurons. *Nature Neuroscience*. 15:1007-1014.
3. Schmidt-Hieber C, Bischofberger J (2010): Fast sodium channel gating supports localized and efficient axonal action potential initiation. *The Journal of Neuroscience.* 30:10233-10242.
4. Garrido JJ, Fernandes F, Giraud P, Mouret I, Pasqualini E, Fache MP, et al. (2001): Identification of an axonal determinant in the C-terminus of the sodium channel Na(v)1.2. *Embo Journal*. 20:5950-5961.
5. Lemaillet G, Walker B, Lambert S (2003): Identification of a conserved ankyrin-binding motif in the family of sodium channel alpha subunits. *The Journal of Biological Chemistry*. 278:27333-27339.